

Identification and optimization of 2-aminobenzimidazole derivatives as novel inhibitors of TRPC4 and TRPC5 channels

Yingmin Zhu^{a,#}, Yungang Lu^{a,b,#,¶}, Chunrong Qu^c, Melissa Miller^{d,¶}, Jinbin Tian^a,
Dhananjay P. Thakur^a, Jinmei Zhu^c, Zixin Deng^c, Xianming Hu^c, Meng Wu^{d,¶}, Owen B.
McManus^{d,¶}, Min Li^{d,¶}, Xuechuan Hong^{c,*}, Michael X. Zhu^{a,*}, Huai-Rong Luo^{c,*},

^a Department of Integrative Biology and Pharmacology, The University of Texas Health Science Center at Houston, Houston, TX, 77030, USA

^b The Third Affiliated Hospital of Guangzhou Medical University, Guangzhou, 510150, China

^c State Key Laboratory of Virology, Key Laboratory of Combinatorial Biosynthesis and Drug Discovery (Wuhan University), Ministry of Education, Wuhan University School of Pharmaceutical Sciences, Wuhan 430071, China

^d Department of Neuroscience, High Throughput Biology Center and Johns Hopkins Ion Channel Center, Johns Hopkins University School of Medicine, Baltimore, Maryland, 21205, USA

^e State Key Laboratory of Phytochemistry and Plant Resources in West China, Kunming Institute of Botany, the Chinese Academy of Sciences, Kunming, Yunnan, China

Running title: Novel 2-aminobenzimidazole-based TRPC4/C5 inhibitors

[#] Equal contribution authors

*Corresponding authors: Dr. Michael X. Zhu, Dr. Xuechuan Hong, and Dr. Huai-Rong Luo

Department of Integrative Biology and Pharmacology
The University of Texas Health Science Center at Houston
6431 Fannin St, MSB 4.128
Houston, TX, 77030, USA
Phone: 713-500-7505

E-mail: michael.x.zhu@uth.tmc.edu; xhy78@whu.edu.cn; luohuirong@mail.kib.ac.cn

This article has been accepted for publication and undergone full peer review but has not been through the copyediting, typesetting, pagination and proofreading process, which may lead to differences between this version and the Version of Record. Please cite this article as doi: 10.1111/bph.13140

†Current affiliations: University of California at Los Angeles (YL), University of California at Berkeley (MM), High-Throughput Screening Facility, University of Iowa (MW), Essen Bioscience (OM), GlaxoSmithKline (ML)

Author contributions

OM, ML, X Hong, HRL, and MXZ designed the research; YZ, YL, CQ, MM, JT, DPT, JZ, ZD, X Hu, MW performed experiments; YZ, YL, MM, JT, MW, OM, X Hong, MXZ, HRL performed data analyses; YZ, YL, MW, OM, ML, X Hong, HRL, and MXZ wrote the paper.

Abbreviations used:

ACPD, (1S,3R)-1-aminocyclopentane-1,3-dicarboxylic acid; 2APB, 2-aminoethoxydiphenyl borate; $[Ca^{2+}]_i$, intracellular Ca^{2+} concentration; CCh, Carbachol; cpd, compound; DHPG, (S)-3,5-dihydroxyphenylglycine (DHPG); DRG, dorsal root ganglion; FBS, fetal bovine serum; FFA, flufenamic acid; FMP, FLIPR membrane potential dye; FMP II, FLIPR membrane potential dye II; GPCR, G protein-coupled receptor; 5-HT, 5-hydroxytryptamine; 5-HT_{1A}R, 5-HT receptor type 1A; I-V, current-voltage; M₂R and M₅R, M₂ and M₅ muscarinic receptor, respectively; MLPCN, Molecular Libraries Probe Production Centers Network; MLSMR, Molecular Libraries Small Molecule Repository; μ OR, μ -opioid receptor; PLC, phospholipase C; SAR, Structure and activity relationship; TRP, Transient Receptor Potential; TRPC, TRP canonical

Abstract:

Background and Purpose: Transient receptor potential canonical (TRPC) channels play important roles in a broad array of physiological functions and are implicated in diseases. However, the lack of potent subtype-specific inhibitors has limited delineation of the roles of TRPC channels in physiological and pathophysiological conditions.

Experimental approach: Using fluorescence membrane potential and Ca^{2+} assays and electrophysiological recording, we characterized new 2-aminobenzimidazole-based small molecular inhibitors of TRPC4 and TRPC5 channels identified from cell-based fluorescence high throughput screening.

Key Results: The original compound, **M084**, had IC_{50} values of 10.3 and 8.2 μM against TRPC4 and TRPC5, respectively, but was also weakly inhibitory to TRPC3 ($\text{IC}_{50} \sim 50 \mu\text{M}$). Structure modifications of the lead compound resulted in the identification of structural analogs with improved potency ($\text{IC}_{50} < 5 \mu\text{M}$) and selectivity for TRPC4 and TRPC5 channels. The aminobenzimidazole derivatives exhibited fast action on inhibiting TRPC4 and TRPC5 currents when applied from the extracellular side and the inhibition was independent of the mode of activation of these channels. The compounds effectively blocked the plateau potential mediated by TRPC4-containing channels in mouse lateral septal neurons but did not affect the activity of heterologously expressed TRPA1, TRPM8, TRPV1, or TRPV3 channels as well as that of the native voltage-gated Na^+ , K^+ and Ca^{2+} channels in dissociated neurons.

Conclusions & Implications: The TRPC4/C5-selective inhibitors developed here represent novel and useful pharmaceutical tools for investigation of physiological and pathophysiological functions of TRPC4/C5 channels.

INTRODUCTION

The superfamily of Transient Receptor Potential (TRP) cation channels in mammals consists of six subfamilies: TRPC (canonical), TRPV (vanilloid), TRPM (melastatin), TRPA (ankyrin), TRPP (polycystin), and TRPML (mucolipin) (Montell et al., 2002). TRPC channels are typically activated downstream from stimulation of phospholipase C (PLC) (Plant and Schaefer, 2003; Trebak et al., 2007). However, which step(s) or constituent(s) of the PLC pathway is the most critical for TRPC activation is not well defined. The mammalian TRPC family has seven members, TRPC1-7, and based on sequence similarities, they are separated into four groups: TRPC1, TRPC2, TRPC3/C6/C7, and TRPC4/C5. TRPC2 is a pseudogene in humans. TRPC3/C6/C7 can be directly activated by diacylglycerols (Hofmann et al., 1999). TRPC4/C5 appears to respond to receptors that activate $G_{i/o}$ signaling in addition to the $G_{q/11}$ -PLC pathway (Jeon et al., 2012; Jeon et al., 2008; Kim et al., 2014; Otsuguro et al., 2008). Because PLC activation is commonly achieved by the stimulation of G protein-coupled receptors (GPCRs) or receptor tyrosine kinases, the TRPC channels are also referred to as receptor-operated channels (Plant and Schaefer, 2003).

Functionally, TRPC channels are non-selective cation channels that mediate Na^+ and Ca^{2+} entry into cells, leading to membrane depolarization and intracellular Ca^{2+} concentration ($[Ca^{2+}]_i$) elevation. The rise in Na^+ level at the cytoplasmic side could also be important for Na^+ -dependent transport (Eder et al., 2005). However, because of the lack of pharmacological tools, the TRPC-mediated physiological functions are often revealed by the studies of TRPC mutant animals or human patients who bear naturally occurring mutations in TRPC genes. These studies have generated a long list of TRPC-dependent functions, including neurotransmission, fear response, and neurodegeneration in the nervous system (Munsch et al., 2003; Phelan et al., 2012; Riccio et al., 2009; Riccio et al., 2014), excitation and contraction coupling and muscle tone of smooth muscles (Tsvilovskyy et al., 2009; Welsh et al., 2002), as well as regulation of endothelial permeability in the vasculature and filtration in the kidney (Tiruppathi et al., 2002; Winn et al., 2005). Currently, the roles of TRPC channels in normal and pathological conditions are under extensive investigation.

The scarcity of TRPC probes has severely hampered the characterization of these channels in their assembly, function, and role in pathophysiology. Using a cell-based high-throughput fluorescence assay to screen for TRPC4 probes from the Molecular Libraries Small Molecule Repository (MLSMR) supported by the Molecular Libraries Probe Production Centers Network (MLPCN), we have identified a small group of compounds showing antagonist activity on TRPC4. We have previously reported that **ML204**, a quinoline compound, potently and selectively inhibited TRPC4 with an IC_{50} value of $0.96\ \mu M$ (Miller et al., 2011a). **ML204** was later shown to inhibit visceral pain in a dose-dependent manner (Westlund et al., 2014) and to protect kidney filter function (Schaldecker et al., 2013). Here, we report characterization and optimization of an (amino)benzimidazole-based compound, **M084**, from the same screen. Although not as potent as **ML204**, the **M084** series affords improved stability and kinetics of inhibiting

TRPC4/C5 and provides an alternative structural scaffold for further development of more potent TRPC4/C5-selective antagonists.

METHODS

Cell Lines and Cell Culture—HEK293 cells were grown in DMEM (high glucose) supplemented with 10% heat-inactivated fetal bovine serum (FBS), 100 units/ml penicillin, and 100 µg/ml streptomycin at 37 °C, 5% CO₂. The stable cell line that inducibly expresses human TRPA1 and the conditions for induction has been described previously (Hu et al., 2009). Rat TRPV1 was transiently transfected into HEK293 cells seeded in wells of 96-well plates and used for Ca²⁺ assay 20 hrs post-transfection as described (Hu et al., 2004). Stable cell lines that express human TRPC3, or mouse TRPC4β, TRPC5, TRPC6, TRPC7, TRPV3, or TRPM8 were established as described previously (Miller et al., 2011a) and maintained in the above medium supplemented with G418 (400 µg/ml; Invitrogen). The stable cell lines over-expressing TRPC4 and TRPC5 were also co-expressed with µ-opioid receptor (µOR) or serotonin 5-HT_{1A} receptor (5-HT_{1A}R). The TRPC6 cell line also stably expressed the M₅ muscarinic receptor (M₅R). For all GPCRs, the receptor cDNA was placed in the pIRESHyg2 vector (Clontech) and the cell lines stably coexpressing TRPC and GPCR were maintained in the medium containing 400 µg/ml G418 and 50 µg/ml hygromycin B (Calbiochem). For the stable cell line co-expressing TRPC1 and TRPC4, human TRPC1 cDNA was placed in a modified pIRESneo vector (Clontech) with the neomycin-resistant gene replaced by the zeocin-resistant one and transfected to the stable cell line that expressed TRPC4β and M₂ muscarinic receptor (M₂R). The cells were maintained in 100 µg/ml zeocin (Invitrogen), in addition to G418 and hygromycin B. The nomenclature for receptors and ion channels conforms to BJP's Concise Guide to Pharmacology (Alexander et al., 2013a, 2013b).

Fluorescence Ca²⁺ and Membrane Potential Assays—HEK293 cells stably expressing the desired channel and receptor types were seeded in wells of 96-well plates pre-coated with polyornithine (20 µg/ml, molecular weight >30,000; Sigma) at 1 X 10⁵ cells/well and grown for >16 hrs. Cells were loaded with either Fluo 4-AM to monitor intracellular Ca²⁺ changes or the FLIPR membrane potential dye (FMP, Molecular Devices) to monitor membrane potential changes by using the FlexStation microplate reader (Molecular Devices) following previously described protocols (Hu et al., 2004; Otsuguro et al., 2008). Either the original FMP or FLIPR membrane potential dye II (FMP II) was used. Extracellular solution for all FlexStation assays contained (in mM) 140 NaCl, 5 KCl, 2 CaCl₂, 1 MgCl₂, 10 glucose, and 10 HEPES, with pH adjusted to 7.4 by NaOH. Probenecid (2 mM) was included in all Ca²⁺ assays except for TRPV1. Assays were run at the 32 °C, except for TRPV1 and TRPA1, which were carried out at the room temperature (~22 °C).

Electrophysiological Recordings—HEK293 cells stably expressing desired TRPC channels were seeded in 35-mm dishes one day before whole-cell recordings were performed. Recording pipettes were pulled from standard wall borosilicate tubing with filament (Sutter Instrument) to 2–4 MΩ when filled with a pipette solution containing (in mM) 110 CsCl, 1 MgCl₂, 6.46 CaCl₂, 10 BAPTA, (with the estimated free [Ca²⁺] of ~400 nM), 10 HEPES, with the pH adjusted to 7.2 with CsOH, and placed in the bath solution

of the same composition as the extracellular solution used for the Ca^{2+} assay. Isolated cells were voltage-clamped in the whole-cell mode using an EPC9 (HEKA Instruments) amplifier. Voltage commands were made from the PatchMaster program (version 2.60; HEKA), and currents were recorded at 5 kHz. Voltage ramps of either 200 or 500 ms to -100 mV after a brief (20-ms) step to +100 mV from holding potential of 0 mV were applied every 1 or 2 s. Cells were continuously perfused with the bath solution through a gravity-driven multi-outlet device with the desired outlet placed about 50 μm away from the cell being recorded. Drugs were diluted in the extracellular solution to the desired final concentrations and applied to the cell through perfusion.

All animal procedures were carried out in accordance with the Guide for the Care and Use of Laboratory Animals as adopted and promulgated by the U.S. National Institutes of Health. The use of mice and animal protocols were approved by the Animal Welfare Committee of The University of Texas Health Science Center at Houston. Preparation of mouse brain slices and recordings of agonist-evoked plateau potential from lateral septal neurons in brain slices by whole-cell current clamp methods were described previously (Tian et al., 2014).

Isolation of mouse dorsal root ganglion (DRG) neurons and whole-cell recordings to test the effects of the compound on voltage-gated Na^+ , K^+ , and Ca^{2+} channels in isolated DRG neurons were essentially carried out as previously described (Miller et al., 2011a). For Na^+ channels, the pipette solution had (in mM): 140 CsCl, 5 NaCl, 4 MgCl_2 , 10 HEPES, 10 EGTA, 2 Na-ATP, 10 HEPES, pH 7.2; bath had: 35 NaCl, 110 choline-Cl, 1.2 MgCl_2 , 0.15 CaCl_2 , 0.2 CdCl_2 , 10 glucose, 10 HEPES, pH 7.4. For K^+ channels, the pipette solution had (in mM): 130 K-methanesulfonate, 7 KCl, 0.05 EGTA, 1 Na_2ATP , 3 MgATP , 0.5 Na_2GTP , 10 HEPES, pH 7.2; bath had: 140 mM choline-Cl, 5 KCl, 2 CoCl_2 , 1 MgCl_2 , 10 glucose, 10 HEPES, pH 7.4. For Ca^{2+} channels (in mM): pipette solution had (in mM): 117 CsCl, 1.8 MgCl_2 , 9 EGTA, 14 Tris-creatine phosphate, 4 MgATP , 0.3 TrisGTP, 9 HEPES, pH 7.2; bath had: 130 tetraethylammonium-Cl, 10 BaCl_2 , 1 MgCl_2 , 0.0004 tetrodotoxin, 10 glucose, 10 HEPES, pH 7.4. Voltage protocols are shown in the figure.

Compounds and Combinatorial Chemical Library Synthesis—A series of novel 2-aminobenzimidazole derivatives were prepared as reported previously (Zhu et al., 2013). Most of the compounds were synthesized from the commercially available 2-chloro-1*H* benzo[*d*]imidazole and amines using methyl-1-butanol or MeOH as the solvent under microwave irradiation. A small number of compounds were purchased from the Sigma-Aldrich and ChemBridge. The structures and sources of all compounds tested in the current study are listed in Table 1. 2-Amino-6-(trifluoromethoxy)benzothiazole (Riluzole) was from Matrix Scientific. Capsaicin, carbamoylcholine (carbachol or CCh), [D-Ala², N-Me-Phe⁴, Gly⁵-ol]-Enkephalin (DAMGO), flufenamic acid, 5-hydroxytryptamine (5-HT), menthol were from Sigma-Aldrich. 2-Aminoethoxydiphenyl borate (2APB) was from Cayman Chemical Co.

RESULTS:

M084 selectively inhibits TRPC4 and TRPC5 — Using a stable HEK293 cell line co-expressing mouse TRPC4 β and μ opioid receptor (μ OR), we conducted high throughput screening for compounds that affect TRPC4 channel function by measuring μ agonist, DAMGO-evoked intracellular Ca^{2+} rise (Miller et al., 2011a; Miller et al., 2011b). One of the primary hits (CID 284016) identified from the screening of a total of 305,000 compounds in the MLSMR library is *n*-butyl-1h-benzimidazol-2-amine (**M084**, Fig. 1E inset). The compound was resynthesized and tested for activity on TRPC4 β stably co-expressed with μ OR using the Ca^{2+} assay (Fig. 1A), from which the IC_{50} was estimated to be $3.7 \pm 0.5 \mu\text{M}$ ($n = 10$) when DAMGO was used at $0.1 \mu\text{M}$. Using the same cell line, we also performed a fluorescence membrane potential assay, which represents a different assay from the primary screening. As shown in Fig. 1B, with the cells loaded with the FLIPR membrane potential dye (FMP), DAMGO ($0.1 \mu\text{M}$) induced a robust increase in fluorescence intensity in the TRPC4 + μ OR cells, indicating membrane depolarization. This response was specific for μ OR-mediated TRPC4 activation as DAMGO failed to induce fluorescence increases in cells that expressed either TRPC4 β or μ OR alone or wild type HEK293 cells (data not shown, but see (Miller et al., 2011b)). Preincubation with **M084** did not cause an appreciable change in the fluorescence signal but attenuated the DAMGO-evoked increase in a concentration dependent manner ($\text{IC}_{50} = 10.3 \pm 0.5 \mu\text{M}$, $n = 12$, Table 2). Similarly, in cells that co-expressed TRPC4 β with serotonin (5-hydroxytryptamine, or 5-HT) receptor type 1A (5-HT $_{1A}$ R), the 5-HT ($1 \mu\text{M}$) evoked fluorescence increase was also inhibited by preincubation of **M084** (Fig. 1C). In addition, **M084** inhibited carbachol (CCh, $1 \mu\text{M}$) evoked membrane depolarization in cells that co-expressed TRPC1, TRPC4 β and M $_2$ R in a concentration-dependent manner (Fig. 1D), with an estimated IC_{50} of $8.3 \pm 1.7 \mu\text{M}$ ($n = 6$), suggesting that the compound also acts on the TRPC1/C4 heteromeric channels. In whole-cell voltage clamp recordings, co-application of DAMGO ($0.1 \mu\text{M}$) and CCh ($10 \mu\text{M}$), which acts at endogenous $\text{G}_{q/11}$ -coupled muscarinic receptors to facilitate TRPC4 current triggered through stimulation of $\text{G}_{i/o}$ signaling, to the TRPC4 β / μ OR co-expressing cells elicited a double rectifying current with an “N-shaped” current-voltage (I-V) relationship, typical for TRPC4/C5 currents (Fig. 1E). Application of **M084** ($8 \mu\text{M}$) immediately decreased the currents, which recovered only moderately and slowly upon washout of **M084** (Fig. 1E). These results confirmed that **M084** is an inhibitor of the TRPC4-containing channels.

TRPC5 is a close homolog of TRPC4 but it shows constitutive activity when expressed in HEK293 cells (Yamada et al., 2000; Zeng et al., 2004). The application of **M084** to cells that stably co-expressed TRPC5 and μ OR immediately led to decreases in fluorescence intensity in a concentration dependent manner in the membrane potential assay (Fig. 2A), indicative of blockade of TRPC5 basal activity in these cells. At the highest concentration tested ($22 \mu\text{M}$), **M084** also inhibited the DAMGO-induced fluorescence increase, but at lower concentrations, the inhibitory effect was not obvious. In fact, lower concentrations of **M084** actually increased the DAMGO-evoked fluorescence increase (Fig. 2A, see 0.8 , 2.5 , and $7.4 \mu\text{M}$ **M084**), likely because the partial inhibition of the constitutive currents produced a lower membrane potential preceding the DAMGO addition. Overall, these data suggest that **M084** also inhibits TRPC5. Supporting this conclusion, **M084** ($8 \mu\text{M}$) caused an immediate inhibition of DAMGO/CCh-evoked whole-cell current in cells that

co-expressed TRPC5 and μ OR (Fig. 2B). On the other hand, **M084** caused weak inhibition of TRPC3 and even more moderate inhibition of TRPC6, as shown by CCh-induced membrane depolarization in cells that stably expressed human TRPC3 alone or mouse TRPC6 together with the $G_{q/11}$ -coupled M_5 muscarinic receptor (M_5R) (Fig. 2C, 2D). The M_5R was introduced because the stable monoclonal TRPC6 cell line had a poor response to CCh as compared to the wild type HEK293 cells (data not shown). These data indicated that among the related TRPC channels, **M084** is relatively selective to TRPC4 and TRPC5. **M084** exhibited a very good solubility in aqueous buffers and was relatively quick with its inhibitory action on these channels. However, the potency of **M084** was low, with IC_{50} values of 10.3 ± 0.5 and 8.2 ± 0.7 μ M for TRPC4 and TRPC5, respectively, as determined by the FMP assay using DAMGO to stimulate $G_{i/o}$ via the co-expressed μ OR (Table 2). In addition, **M084** displayed a weak but clear inhibitory effect on TRPC3, with an IC_{50} of ~ 50 μ M (Table 2). Therefore, we searched and synthesized structural analogs of **M084** in order to identify more potent and selective inhibitors for TRPC4 and/or TRPC5.

Structure and activity relationship (SAR) of M084 — We have tested a total of 28 structural analogs of **M084**, obtained either from commercial sources or through new synthesis (Table 1), against the TRPC4 β / μ OR cells using the FMP assay. The results revealed that the amino group linked to position 2 of the benzimidazole backbone was absolutely required for activity. This could be either a primary (**M084** and compound **27**) or secondary amine in the form of a ring structure either as a piperidine (compounds **9**, **13**, **16**, and **28**) or a pyrrolidine (**17**). Therefore, the 2-aminobenzimidazol skeleton forms the basic scaffold required for inhibiting TRPC4. Generally, a carbonyl functional group and π system were not well tolerated at the amino position of benzimidazole, as indicated by for example, acylation (**4** and **10**), aromatic substitution (**7**, **18**, **25**, and **29**), or addition of alcohol or ether (**3** and **22**) or the substituted morpholine (**15**); neither was an additional amine, such as the aliphatic heteroalkane chains on the amino position (**23** and **24**) and the substituted piperazine (**11** and **12**), tolerated. Dialkylation of the amine (**20**, **21**, and **25**) also resulted in the loss of function on TRPC4. Pyrrolidine and methylpiperidine at position 2 of the benzimidazole backbone appeared to work slightly better than the original *n*-butylamine, suggesting that the *n*-butyl chain might loop around to interact with the channel. This is supported by the inhibitory action of compound (cpd) **27**, in which the primary amine is sterically hindered. However, the piperidine has to be linked with the benzimidazole backbone via the amino group (**16**) instead of an alkyl group (**14**), further emphasizing the essential scaffold being the 2-aminobenzimidazole. The methyl group of the methylpiperidine could be added at either the 4th (**9** and **13**) or the 2nd position (**28**) of the piperidine. Modifications at position 1 of the benzimidazole backbone tended to reduce the inhibitory effect on TRPC4 (e.g. cpds **8** and **19**), while substitution of the proton with Cl⁻ at position 5 of the benzimidazole backbone was well tolerated (compare cpds **9** and **13**).

We have determined the IC_{50} values for cpds **9**, **13**, **16**, **17**, **27**, and **28** on DAMGO-induced depolarization in cells that co-expressed TRPC4 β and μ OR (Fig. 3A and Table 2). Cpds **9**, **13**, **17**, and **28** showed improved potency over the original compound, with about 50% decrease in IC_{50} values. Similar improvement was also found for cpds **9**, **13**, and **28** against TRPC5 activated by DAMGO through the co-expressed μ OR (Table 2).

However, both cpd **9** and cpd **13** still showed weak inhibition on TRPC3 and slight inhibition on TRPC6 at high concentrations (Table 2). On the other hand, cpds **16**, **17**, **27** and **28** did not inhibit TRPC3 or C6 (Table 2). Cpd **28** also inhibited CCh-evoked membrane depolarization in cells that co-expressed TRPC1, TRPC4 β and M₂R (Fig. 3D), with an estimated IC₅₀ of $11.0 \pm 1.7 \mu\text{M}$ ($n = 6$). Although the IC₅₀ value did not improve from **M084**, the analog cpd **28** did not induce the slow depolarization seen with the high concentration of **M084** on the TRPC1/C4 heteromeric channel (compare 22.2 μM traces between Fig. 1D and Fig. 3D). In addition, cpd **28** did not affect CCh-induced Ca²⁺ response in wild type HEK293 cells (Fig. 3H) and it did not inhibit CCh-evoked membrane depolarization through TRPC7 (Fig. 3G). Example traces for cpd **28** effects on TRPC3, C4, C1/C4, C5, C6, and C7, as measured by agonist-evoked membrane depolarization using the FLIPR membrane potential dye II (FMP II) are shown in Fig. 3B-3G. Note that FMP II exhibited slower kinetics and gave smaller fold fluorescence increases in response to TRPC channel-mediated membrane depolarization than the original FMP dye; however, it also yielded less fluorescence decrease upon inhibition of the constitutive activity of TRPC5 in response to application of the antagonist (compare Fig. 2A and Fig. 3C).

In whole-cell recordings, acute application of cpd **28** (10 μM) led to inhibition of TRPC4 β currents activated by co-stimulation of G_{i/o} and G_{q/11} pathways with DAMGO (0.1 μM) plus CCh (30 μM) in cells that co-expressed TRPC4 β and μOR (Fig. 4A). It also inhibited TRPC5 currents activated by CCh (100 μM) via endogenous muscarinic receptors in the TRPC5-expressing cells (Fig. 4B). Note the much smaller inward currents at negative potentials for TRPC5 in the absence of G_{i/o} stimulation. For both TRPC4 and TRPC5, the inhibition by cpd **28** was more pronounced at negative than at positive potentials (Fig. 4C-4F). Quantification of the degree of inhibition by cpd **28** at -100 mV and +100 mV revealed 83.4 ± 4.1 and $48.9 \pm 8.6\%$ reduction of TRPC4 and 86.8 ± 3.5 and $62.7 \pm 4.8\%$ reduction of TRPC5 currents, respectively (Fig. 4E, 4F). Similar inhibition of TRPC4 and TRPC5 currents were also observed with the acute application of cpds **9** and **13** (Fig. 4E, 4F). Recently, riluzole was shown to activate TRPC5 independent of receptor/PLC activation (Richter et al., 2014a). Application of cpd **28** (10 μM) also caused instantaneous inhibition of riluzole-evoked TRPC5 current (Fig. 4G). In addition, in the TRPC1/C4/M₂R coexpressing cells, cpd **28** (10 μM) also strongly depressed the current evoked by CCh.

Pre-exposure of the cells to cpd **28** for ~30 sec also strongly inhibited the activation of TRPC4 β by the co-stimulation of DAMGO and CCh by ~80 and 98% at +100 and -100 mV, respectively (Fig. 5A-5C). Similarly, pretreatment with cpd **28** also blocked the CCh-evoked TRPC5 currents by ~85 and 90% at +100 and -100 mV, respectively (Fig. 5D-5F). Noticeably, bath application of cpd **28** also reduced the constitutive outward current in TRPC5-expressing cells (Fig. 5E), consistent with the observation in fluorescence membrane potential measurements (Fig. 3C). By contrast, pretreatment with cpd **28** did not significantly alter the CCh-evoked TRPC6 currents in cells that co-expressed TRPC6 and M₅R (Fig. 5G-5I), confirming the lack of its effect on TRPC6. Therefore, the results from the electrophysiological experiments corroborate the conclusions from the fluorescence membrane potential assay that cpds **9**, **13**, and **28** are TRPC4/C5 blockers and cpd **28** has an improved selectivity over **M084** on the

TRPC4/C5 subgroup of TRPC channels. The fast onset of action of these drugs makes them ideally suited in electrophysiological experiments to isolate currents mediated by native TRPC4/C5 channels.

M084 and its analogs have minimal effect on related channels — Using stable cell lines that expressed TRPA1, TRPM8, TRPV1, and TRPV3 channels, we examined the effects of **M084** and a selected number of its analogs, cpds **9**, **13**, **27** and **28**, on these distantly related TRP channels. The cells were loaded with Fluo-4 and then stimulated with the respective agonist for each channel, with changes in $[Ca^{2+}]_i$ monitored by a fluorescence plate reader. As exemplified in Fig. 6A-6D for cpd **28** and summarized in Fig. 6E for all five compounds, **M084** and cpds **9**, **13**, and **28** showed neither agonistic nor antagonistic effect on the tested TRP channels. Cpd **27** was ineffective on TRPV1 and TRPV3, but moderately inhibited TRPA1 and TRPM8. The inhibition on TRPM8 was not very surprising as a number of benzimidazole-containing compounds have been shown to be potent antagonists of TRPM8 (Parks et al., 2011; Calvo et al., 2012). Furthermore, using freshly isolated mouse DRG neurons, we recorded native voltage-gated Na^+ , K^+ , and Ca^{2+} currents and found that **M084** had no effect on these channels (Fig. 6F). These data further confirm the selectivity of the **M084** compound series on TRPC, especially TRPC4/C5 channels.

M084 and its analogs inhibit native TRPC4-like activity in lateral septal neurons — We and others have shown that TRPC4-containing channels mediate a plateau potential response when stimulated by the agonist of group I metabotropic glutamate receptors, (S)-3,5-dihydroxyphenylglycine (DHPG) or (1S,3R)-1-aminocyclopentane-1,3-dicarboxylic acid (ACPD), in rodent lateral septal neurons (Phelan et al., 2012; Tian et al., 2014). This response was greatly facilitated by the injection of a positive current while DHPG (30 μ M) was applied (Fig. 7A). While co-application of the previously reported TRPC4/C5 blocker, ML204 (30 μ M), significantly suppressed the DHPG-induced plateau depolarization (Fig. 7B, 7G), the inhibition was incomplete, probably because of the slow mechanism of action and the relatively poor aqueous stability of the compound. On the other hand, when coapplied without preincubation, **M084** (100 μ M) and its analogs, cpds **9**, **13** and **28** (all at 30 μ M), inhibited the DHPG-induced plateau depolarization by ~80% (Fig. 7C-7G), demonstrating the effectiveness of these blockers in acute suppression of native TRPC4-containing channels, in agreement with their actions on heterologously expressed channels.

DISCUSSION & CONCLUSIONS

Small molecular probes for TRPCs are of critical value for analyzing physiological and pathophysiological functions of these channels. Because of the lack of specific inhibitors, testing of native TRPC channel functions has been limited to the use of nonspecific blockers, such as SKF96365 and 2-aminoethoxydiphenyl borate (2APB) and occasionally flufenamic acid (Hu et al., 2004; Inoue et al., 2001; Merritt et al., 1990). However, these compounds have low potency on TRPC channels and are either equally effective or better at against other non-TRPC targets (Merritt et al., 1990; Singh et al., 2010). Therefore,

several groups have made efforts to identify novel small molecular probes for TRPC channels (Kiyonaka et al., 2009; Majeed et al., 2011; Miede et al., 2012; Miller et al., 2011a; Schleifer et al., 2012; Urban et al., 2012; Washburn et al., 2013; Richter et al., 2014a, 2014b). Previously, we have reported the characterization of **ML204** as a selective inhibitor of TRPC4/C5 (Miller et al., 2011a). Others have found **ML204** to be useful in demonstrating the functions of native TRPC4 and/or TRPC5 channels in visceral pain (Westlund et al., 2014), disruption of kidney filtration barrier (Schaldecker et al., 2013), and neuronal excitability regulation (Zhang et al., 2013; Kolaj et al., 2014).

The **M084** series reported here represents a different hit from the same screen that identified **ML204**, in which a cell-based assay was used to monitor DAMGO-evoked $[Ca^{2+}]_i$ rise via mouse TRPC4 β by activation of the co-expressed $G_{i/o}$ -coupled μ OR (Miller et al., 2011a; Miller et al., 2011b). The primary hit, **M084**, contains a 2-aminobenzimidazole scaffold. Through SAR studies, we have shown the amine at the 2nd position of benzimidazole being essential for the inhibitory action on TRPC4, indicating that indeed the basic structural backbone for this series is 2-aminobenzimidazole. This differs from the series of benzimidazole-containing antagonists for TRPM8, in which an amino group is typically not present at such position (Parks et al., 2011; Calvo et al., 2012). However, just the 2-aminobenzimidazole backbone itself (cpd **2**) exhibited no activity on TRPC4. The addition of a four-carbon alkyl radical (*n*-butyl) or the joining of the amine by four or five carbons to form pyrrolidine or piperidine, respectively, was necessary to confer the inhibition on TRPC4. This suggests that a ring-shaped structure around the amine may be important for binding to and/or the inhibitory action on the TRPC channel. It is possible that the *n*-butyl chain of **M084** also loops around to form a pseudo “ring-shaped” structure when binding to the channel. This explains the lower apparent affinity of **M084**, based on the IC_{50} value, than its analogs with the pyrrolidine or piperidine substitution. Yet, we found that methylpiperidine worked better than piperidine in this position. Although addition of the methyl group at either the 2nd or the 4th position of the piperidine worked equally well on TRPC4 and C5, the methyl group at the 4th position seems to confer some activity, albeit weak, on TRPC3 and TRPC6. Thus, without the methyl at the 4th position, cpds **16**, **17**, and **28** did not show appreciable inhibition on TRPC3 and TRPC6 at 22 μ M. Also interesting is that although the substitution of the *n*-butylamine with a sterically hindered primary amine (cpd **27**) was allowed, other substitutions, e. g. aromatic structures, acylation, dialkylation, and introduction of alcohol, ether or additional amine, all resulted in the loss of inhibitory action on TRPC4. Therefore, a heterocyclic aliphatic amine attached to the 2nd position of a benzimidazol backbone forms the basic structure for binding to and/or inhibiting TRPC4/C5 channels. The requirement for a heterocyclic aliphatic amine is similar to the SAR profile of **ML204** (Miller et al., 2011a), suggesting that the two compound series may share a similar mechanism of action. Therefore, even though the original hits **ML204** and **M084** did not look alike, the inhibitory action on TRPC channels probably involves pyrrolidine- or piperidine-like structures with a methyl group allowed at certain positions. The quinoline (**ML204**) and benzimidazol (**M084**) backbones are probably not essential for binding to the channels and the inhibitory action, but may influence the compound stability and its kinetics for interaction with the channels.

The **M084** series was found to inhibit homomeric TRPC4 and TRPC5 as well as heteromeric TRPC1/C4 channels in both the fluorescence membrane potential assay and whole-cell voltage clamp recordings. The inhibition was not dependent on the receptor type employed to trigger channel activation. Importantly, not only the activation of TRPC4 or TRPC5 by the $G_{i/o}$ -coupled μ OR or 5-HT_{1A}R, but also that of TRPC5 by the endogenous $G_{q/11}$ -coupled muscarinic receptors, as well as its direct agonist, riluzole, was inhibited by **M084** and its analogs. Furthermore, the constitutive activity of TRPC5 was reduced by these compounds in both the fluorescence membrane potential and electrophysiological assays. These, together with the finding that only some, but not all of these inhibitors weakly blocked $G_{q/11}$ -mediated activation of TRPC3 and TRPC6, suggest a direct inhibitory effect of the aminobenzimidazole compounds on TRPC4/C5 channels.

We found **M084** and its analogs to be relatively selective to TRPC, especially TRPC4/C5, channels. At the highest concentration tested (22 μ M), these compounds did not affect the functions of TRPA1, TRPM8, TRPV1, and TRPV3 heterologously expressed in HEK293 cells in Ca^{2+} influx assays. In whole-cell recordings of mouse DRG neurons, **M084** did not significantly alter the current density of voltage-gated Na^+ , K^+ , or Ca^{2+} channels. Importantly, unlike **ML204** (Miller et al., 2011a), cpd **28** did not affect intracellular Ca^{2+} release induced through activation of endogenous muscarinic receptors. Among the analogs analyzed here, cpd **28** yielded low IC_{50} values against TRPC4 and TRPC5 and showed no inhibitory effect on TRPC3/C6/C7, indicating that it is an excellent TRPC4 and TRPC5 selective inhibitor. In electrophysiological recordings, all aminobenzimidazole compounds produced immediate inhibition of TRPC4 and TRPC5 currents following bath application, indicating a direct and fast action by the compounds. This feature is particularly important in electrophysiological studies to determine the contribution of native TRPC4/C5 channels. Indeed, recordings of DHPG-induced plateau potential in mouse lateral septal neurons demonstrated the effectiveness of **M084** and its analogs, cpds **9**, **13** and **28**, on inhibiting native TRPC4-containing channels. Under the conditions used for these experiments, the **M084** series exhibited better inhibitory effect than **ML204**, suggesting improved stability and/or action kinetics. Curiously, however, we have found that cpds **16** and **28** blocked butyrylcholinesterase in a cell-free assay at similar to or slightly better potency than their inhibition of TRPC4 or TRPC5 functions (Zhu et al., 2013). A recent study also showed that **ML204** inhibited acetylcholinesterase in the cell-free assay at similar potency as its inhibition of TRPC4 (Antolín and Mestres, 2015). Although the cholinesterases are not known to regulate TRPC channels, cautions should be taken when using these compounds to study native TRPC4/C5 function in the presence of cholinesterase activities. Since cpd **27** exhibited no effect on cholinesterases (Zhu et al., 2013), it may be used as an alternative or an additional control to confirm the involvement of TRPC4/C5 channels. However, other off-target effects of cpd **27**, e.g. TRPA1 and TRPM8, should also be carefully evaluated before a conclusion is reached. Further improvements of the aminobenzimidazoles may yield compounds with higher potency and better selectivity against TRPC4 and/or TRPC5.

Pharmacological tools are essential for revealing the function of TRP channels. Currently available compounds tend to broadly affect voltage-gated channels, intracellular Ca^{2+} release channels, chloride channels, and/or multiple types of TRP channels from several

subfamilies (Hofmann et al., 1999; Inoue et al., 2001; Merritt et al., 1990). Therefore, identification of isoform specific probes for TRP channels is important for advancing the studies and understanding on these channels. Because TRPC4/C5 channels are implicated in diseases (Jung et al., 2011; Schaldecker et al., 2013; von Spiczak et al., 2010), the pharmacological tools may also have therapeutic potential. The specific TRPC4/C5 inhibitors reported here should be excellent tools for physiological and pathological studies defining the functional significance of TRPC4/C5-containing channels and may facilitate the development of therapeutics targeting TRPC channels.

Acknowledgements

We thank Dr. Corey Hopkins for initial evaluation of the lead compounds and suggestions on structural analogs. This work was supported by grants from National Institutes of Health (NS056942, NS092377, and DK081654 to MXZ, U54 MH084691 to ML), National Natural Science Foundation of China (81373254 and 21390402 to X. Hong), Natural Science Foundation of Yunnan Province (2012FB181 and 2014BC011 to HRL), postdoctoral fellowship from the Third Affiliated Hospital of Guangzhou Medical University (to YL), predoctoral fellowship from American Heart Association-Southwest Affiliate (to DPT), Fundamental Research Funds for the Central Universities (to CQ), and Innovation Seed Fund of Wuhan University School of Medicine (to X Hong).

Conflicts of Interest

None.

REFERENCES

- Alexander SP, Benson HE, Faccenda E, Pawson AJ, Sharman JL, Spedding M, *et al.* (2013a). The Concise Guide to PHARMACOLOGY 2013/14: G protein-coupled receptors. *Br J Pharmacol* 170:1459-1581.
- Alexander SP, Benson HE, Faccenda E, Pawson AJ, Sharman JL, Catterall WA, *et al.* (2013b). The Concise Guide to PHARMACOLOGY 2013/14: ion channels. *Br J Pharmacol* 170: 1607-1651.
- Antolín AA, Mestres J (2015). Distant Polypharmacology among MLP Chemical Probes. *ACS Chem Biol* 2014 Nov 6. [Epub ahead of print]
- Calvo RR, Meegalla SK, Parks DJ, Parsons WH, Ballentine SK, Lubin ML *et al.* (2012). Discovery of vinylcycloalkyl-substituted benzimidazole TRPM8 antagonists effective in the treatment of cold allodynia. *Bioorg Med Chem Lett* 22: 1903-1907.
- Eder P, Poteser M, Romanin C, Groschner K (2005). Na⁺ entry and modulation of Na⁺/Ca²⁺ exchange as a key mechanism of TRPC signaling. *Pflugers Arch* 451: 99-104.
- Hofmann T, Obukhov AG, Schaefer M, Harteneck C, Gudermann T, Schultz G (1999). Direct activation of human TRPC6 and TRPC3 channels by diacylglycerol. *Nature* 397: 259-263.
- Hu H, Tian J, Zhu Y, Wang C, Xiao R, Herz JM, *et al.* (2009). Activation of TRPA1 channels by fenamate nonsteroidal anti-inflammatory drugs. *Pflugers Arch* 459: 579-592.
- Hu HZ, Gu Q, Wang C, Colton CK, Tang J, Kinoshita-Kawada M, *et al.* (2004). 2-aminoethoxydiphenyl borate is a common activator of TRPV1, TRPV2, and TRPV3. *J Biol Chem* 279: 35741-35748.
- Inoue R, Okada T, Onoue H, Hara Y, Shimizu S, Naitoh S, *et al.* (2001). The transient receptor potential protein homologue TRP6 is the essential component of vascular α_1 -adrenoceptor-activated Ca²⁺-permeable cation channel. *Circ Res* 88: 325-332.
- Jeon JP, Hong C, Park EJ, Jeon JH, Cho NH, Kim IG, *et al.* (2012). Selective Gai subunits as novel direct activators of transient receptor potential canonical (TRPC)4 and TRPC5 channels. *J Biol Chem* 287: 17029-17039.
- Jeon JP, Lee KP, Park EJ, Sung TS, Kim BJ, Jeon JH, *et al.* (2008). The specific activation of TRPC4 by Gi protein subtype. *Biochem Biophys Res Commun* 377: 538-543.
- Jung C, Gené GG, Tomás M, Plata C, Selent J, Pastor M, *et al.* (2011). A gain-of-function SNP in TRPC4 cation channel protects against myocardial infarction. *Cardiovasc Res* 91: 465-471.
- Kim J, Kwak M, Jeon JP, Myeong J, Wie J, Hong C, *et al.* (2014). Isoform- and receptor-specific channel property of canonical transient receptor potential (TRPC)1/4 channels. *Pflugers Arch* 466: 491-504.

- Kiyonaka S, Kato K, Nishida M, Mio K, Numaga T, Sawaguchi Y, *et al.* (2009). Selective and direct inhibition of TRPC3 channels underlies biological activities of a pyrazole compound. *Proc Natl Acad Sci U S A* 106: 5400-5405.
- Kolaj M, Zhang L, Renaud LP (2014). Novel coupling between TRPC-like and KNa channels modulates low threshold spike-induced afterpotentials in rat thalamic midline neurons. *Neuropharmacology* 86: 88-96.
- Majeed Y, Amer MS, Agarwal AK, McKeown L, Porter KE, O'Regan DJ, *et al.* (2011). Stereo-selective inhibition of transient receptor potential TRPC5 cation channels by neuroactive steroids. *Br J Pharmacol* 162: 1509-1520.
- Merritt JE, Armstrong WP, Benham CD, Hallam TJ, Jacob R, Jaxa-Chamiec A, *et al.*, (1990). SK&F 96365, a novel inhibitor of receptor-mediated calcium entry. *Biochem J* 271: 515-522.
- Miehe S, Crause P, Schmidt T, Löhn M, Kleemann HW, Licher T, *et al.* (2012). Inhibition of diacylglycerol-sensitive TRPC channels by synthetic and natural steroids. *PLoS One* 7: e35393.
- Miller M, Shi J, Zhu Y, Kustov M, Tian JB, Stevens A, *et al.* (2011a). Identification of ML204, a novel potent antagonist that selectively modulates native TRPC4/C5 ion channels. *J Biol Chem* 286: 33436-33446.
- Miller M, Wu M, Xu J, Weaver D, Li M, Zhu MX (2011b). High-Throughput Screening of TRPC Channel Ligands Using Cell-Based Assays, in *TRP Channels* (Zhu MX ed), CRC PressLlc., Boca Raton (FL).
- Montell C, Birnbaumer L, Flockerzi V (2002) The TRP channels, a remarkably functional family. *Cell* 108: 595-598.
- Munsch T, Freichel M, Flockerzi V, Pape HC (2003). Contribution of transient receptor potential channels to the control of GABA release from dendrites. *Proc Natl Acad Sci U S A* 100: 16065-16070.
- Otsuguro K, Tang J, Tang Y, Xiao R, Freichel M, Tsvilovsky V, *et al.* (2008) Isoform-specific inhibition of TRPC4 channel by phosphatidylinositol 4,5-bisphosphate. *J Biol Chem* 283: 10026-10036.
- Parks DJ, Parsons WH, Colburn RW, Meegalla SK, Ballentine SK, Illig CR *et al.* (2011). Design and optimization of benzimidazole-containing transient receptor potential melastatin 8 (TRPM8) antagonists. *J Med Chem* 54: 233-247.
- Phelan KD, Mock MM, Kretz O, Shwe UT, Kozhemyakin M, Greenfield LJ, *et al.* (2012) Heteromeric canonical transient receptor potential 1 and 4 channels play a critical role in epileptiform burst firing and seizure-induced neurodegeneration. *Mol Pharmacol* 81: 384-392.
- Plant TD, Schaefer M (2003). TRPC4 and TRPC5: receptor-operated Ca^{2+} -permeable nonselective cation channels. *Cell Calcium* 33: 441-450.
- Riccio A, Li Y, Moon J, Kim KS, Smith KS, Rudolph U, *et al.* (2009). Essential role for TRPC5 in amygdala function and fear-related behavior. *Cell* 137: 761-772.
- Riccio A, Li Y, Tsvetkov E, Gapon S, Yao GL, Smith KS, *et al.* (2014). Decreased anxiety-like behavior and $\text{G}\alpha_{q/11}$ -dependent responses in the amygdala of mice lacking TRPC4 channels. *J Neurosci* 34: 3653-3667.
- Richter JM, Schaefer M, Hill K (2014a). Riluzole activates TRPC5 channels independently of PLC activity. *Br J Pharmacol* 171: 158-170.

- Richter JM, Schaefer M, Hill K (2014b). Clemizole hydrochloride is a novel and potent inhibitor of transient receptor potential channel TRPC5. *Mol Pharmacol* 86: 514-521.
- Schaldecker T, Kim S, Tarabanis C, Tian D, Hakrrouch S, Castonguay P, *et al.* (2013) Inhibition of the TRPC5 ion channel protects the kidney filter. *J Clin Invest* 123: 5298-5309.
- Schleifer H, Doleschal B, Lichtenegger M, Oppenrieder R, Derler I, Frischauf I, *et al.* (2012). Novel pyrazole compounds for pharmacological discrimination between receptor-operated and store-operated Ca^{2+} entry pathways. *Br J Pharmacol* 167: 1712-1722.
- Singh A, Hildebrand ME, Garcia E, Snutch TP (2010). The transient receptor potential channel antagonist SKF96365 is a potent blocker of low-voltage-activated T-type calcium channels. *Br J Pharmacol* 160: 1464-1475.
- Tian J, Thakur DP, Lu Y, Zhu Y, Freichel M, Flockerzi V, *et al.* (2014) Dual depolarization responses generated within the same lateral septal neurons by TRPC4-containing channels. *Pflugers Arch* 466: 1301-1316.
- Tiruppathi C, Freichel M, Vogel SM, Paria BC, Mehta D, Flockerzi V, *et al.* (2002). Impairment of store-operated Ca^{2+} entry in TRPC4^{-/-} mice interferes with increase in lung microvascular permeability. *Circ Res* 91: 70-76.
- Trebak M, Lemonnier L, Smyth JT, Vazquez G, Putney JW (2007). Phospholipase C-coupled receptors and activation of TRPC channels. *Handb Exp Pharmacol*: 593-614.
- Tsvilovskyy VV, Zholos AV, Aberle T, Philipp SE, Dietrich A, Zhu MX, *et al.* (2009). Deletion of TRPC4 and TRPC6 in mice impairs smooth muscle contraction and intestinal motility in vivo. *Gastroenterology* 137: 1415-1424.
- Urban N, Hill K, Wang L, Kuebler WM, Schaefer M (2012). Novel pharmacological TRPC inhibitors block hypoxia-induced vasoconstriction. *Cell Calcium* 51: 194-206.
- von Spiczak S, Muhle H, Helbig I, de Kovel CG, Hampe J, Gaus V, *et al.* (2010). Association study of TRPC4 as a candidate gene for generalized epilepsy with photosensitivity. *Neuromolecular Med* 12: 292-299.
- Washburn DG, Holt DA, Dodson J, McAtee JJ, Terrell LR, Barton L, *et al.* (2013). The discovery of potent blockers of the canonical transient receptor channels, TRPC3 and TRPC6, based on an anilino-thiazole pharmacophore. *Bioorg Med Chem Lett* 23: 4979-4984.
- Welsh DG, Morielli AD, Nelson MT, Brayden JE (2002). Transient receptor potential channels regulate myogenic tone of resistance arteries. *Circ Res* 90: 248-250.
- Westlund KN, Zhang LP, Ma F, Nesemeier R, Ruiz JC, Ostertag EM, *et al.* (2014). A rat knockout model implicates TRPC4 in visceral pain sensation. *Neuroscience* 262: 165-175.
- Winn MP, Conlon PJ, Lynn KL, Farrington MK, Creazzo T, Hawkins AF, *et al.* (2005). A mutation in the TRPC6 cation channel causes familial focal segmental glomerulosclerosis. *Science* 308: 1801-1804.
- Yamada H, Wakamori M, Hara Y, Takahashi Y, Konishi K, *et al.* (2000). Spontaneous single-channel activity of neuronal TRP5 channel recombinantly expressed in HEK293 cells. *Neurosci Lett* 285:111-4.

Zeng F, Xu SZ, Jackson PK, McHugh D, Kumar B, Fountain SJ, *et al.* (2004). Human TRPC5 channel activated by a multiplicity of signals in a single cell. *J Physiol* 559: 739-750.

Zhang L, Kolaj M, Renaud LP (2013). GIRK-like and TRPC-like conductances mediate thyrotropin-releasing hormone-induced increases in excitability in thalamic paraventricular nucleus neurons. *Neuropharmacology* 72: 106-115.

Zhu J, Wu CF, Li X, Wu GS, Xie S, Hu QN, *et al.* (2013) Synthesis, biological evaluation and molecular modeling of substituted 2-aminobenzimidazoles as novel inhibitors of acetylcholinesterase and butyrylcholinesterase. *Bioorg Med Chem* 21: 4218-4224.

FIGURE LEGENDS

Figure 1 | M084 inhibited agonist-evoked TRPC4 activity. **A-C**, Pretreatment with **M084** inhibited TRPC4-mediated Ca^{2+} influx (**A**) and membrane depolarization (**B**, **C**) in a concentration-dependent manner. HEK293 cells stably co-expressing TRPC4 β and μ opioid receptor (μ OR, **A**, **B**) or 5-hydroxytryptamine (5-HT) 1A receptor (5-HT_{1A}R, **C**) were seeded in wells of 96-well plates, loaded with Flou-4 (**A**) or FLIPR membrane potential dye (FMP, **B**, **C**) and read in a microplate reader. **M084** at different concentrations and buffer alone (0 μM) were added as indicated for 2.5 minutes before DAMGO (0.1 μM , **A**, **B**) or 5-HT (1 μM , **C**) was introduced. Increases in fluorescence intensity indicate intracellular Ca^{2+} elevation (**A**) or membrane depolarization (**B**, **C**). **D**, Similar to **B** and **C**, but cells stably co-expressed TRPC1, TRPC4 β and M₂R. FLIPR membrane potential dye II (FMPII) was used and stimulation was by carbachol (CCh, 1 μM). Because high concentrations of **M084** caused slow fluorescence increase in these cells, the fluorescence changes were normalized to the fluorescence intensity immediately preceding CCh addition (F_{180}) instead of that in the beginning of the experiment (F_0) as in all other examples. The same color code for **M084** concentrations is used for all traces shown in **A-D**. **E**, **M084** inhibited TRPC4 currents. Representative traces showing currents at +100 and -100 mV evoked by coapplication of DAMGO (0.1 μM) and CCh (10 μM) to a cell that co-expressed TRPC4 β and μ OR. **M084** (8 μM) was added as indicated. Currents were elicited by 500-ms voltage ramps from +100 to -100 mV from the holding potential of 0 mV applied every 2 s. Dashed line indicates zero current. Current-voltage (I-V) relationships obtained from the voltage ramps at the time points indicated are shown below the time courses. Inset shows the structure of **M084**. Representative of 7 experiments with similar results.

Figure 2 | M084 inhibited TRPC5 activity and exhibited minimal effects on TRPC3 and TRPC6. **A**, **M084** inhibited basal activity of TRPC5. Similar to Fig. 1**B**, but the fluorescence membrane potential assay was performed using cells that stably co-expressed TRPC5 and μ OR. The addition of **M084** reduced the basal fluorescence in a concentration-dependent manner. **B**, **M084** inhibited TRPC5 currents. Similar to Fig. 1**E**, but for a cell that co-expressed TRPC5 and μ OR and voltage ramps were applied every 1 s. Currents were induced by the coapplication of DAMGO (0.1 μM) and CCh (10 μM). Addition of **M084** (8 μM) in the presence of DAMGO and CCh immediately suppressed the currents, which partially recovered upon washout of **M084**. I-V relationships obtained from the voltage ramps at the time points indicated are shown below the time courses. Representative of 5 experiments with similar results. **C** & **D**, **M084** weakly inhibited TRPC3 (**C**) and TRPC6 (**D**). Similar to Fig. 1**B**, but the fluorescence membrane potential assay was performed using cells that stably expressed human TRPC3 (**C**) or co-expressed mouse TRPC6 and M₅ muscarinic receptor (M₅R, **D**). The addition of **M084** caused little fluorescence change and CCh-evoked membrane depolarization was only weakly inhibited by **M084**. The concentrations of CCh used were 100 μM (**C**) and 0.3 μM (**D**).

Figure 3 | Structural analogs of M084 inhibited TRPC4 and TRPC5. A,

Concentration dependence of **M084** and its structural analogs for inhibition of DAMGO-evoked membrane depolarization in the stable HKE293 cell line that co-expressed TRPC4 β and μ OR. Fluorescence membrane potential assays were performed as in Fig. 1B using the aminobenzimidazole compounds as indicated. DAMGO (0.1 μ M) evoked fluorescence increases (area under the curve) were normalized to that from the control pretreated with the buffer alone. Data are means \pm SEM for $n = 12$ measurements for all compounds. Data points were fitted with the Hill equation. **B-G**, Representative traces of the fluorescence membrane potential assays using FMPII performed on cells that expressed TRPC4 β and μ OR (**B**), TRPC5 and μ OR (**C**), TRPC1, TRPC4 β and M₂R (**D**), TRPC3 only (**E**), TRPC6 and M₅R (**F**), or TRPC7 only (**G**). Compound **28** was applied as indicated and the respective receptor agonist was added 2.5 min later. Receptor agonist concentrations used were: DAMGO, 0.1 μ M (**B** & **C**), CCh, 0.3 μ M (**F**), 1 μ M (**D**) and 100 μ M (**E**, **G**). Note the concentration-dependent suppression of DAMGO-evoked depolarization for TRPC4 β (**B**), TRPC5 (**C**), and TRPC1/C4 (**D**) by compound **28**, as well as the decrease of basal fluorescence for TRPC5-expressing cells (**C**). The compound did not inhibit CCh-evoked response for TRPC3 (**E**), TRPC6 (**F**), and TRPC7 (**G**). **H**, Compound **28** did not affect CCh-evoked Ca²⁺ response in wild type HEK293 cells. Untransfected cells were seeded in wells of a 96-well plate, loaded with Fluo-4 and read in a microplate reader. Compound **28** or buffer alone (0 μ M) was applied as indicated. The addition of CCh (100 μ M) immediately increased fluorescence, indicating a rise in [Ca²⁺]_i, which was unaffected by the pretreatment with the compound. The same color code for compound **28** concentrations is used for all traces shown in **B-H**.

Figure 4 | M084 analogs inhibited agonist-evoked TRPC4 and TRPC5 currents. A,

Compound **28** inhibited TRPC4 currents. Similar to Fig. 1E, but the voltage ramp was 200 ms and repeated every 1 s. Currents were elicited by the coapplication of DAMGO (0.1 μ M) and CCh (30 μ M) in a cell that co-expressed TRPC4 β and μ OR. Compound **28** (10 μ M) was applied as indicated after the currents had developed and this led to immediate decreases of currents at both positive and negative potentials. I-V relationships obtained from the voltage ramps at the time points indicated are shown to the right. **B**, Similar to **A**, but for a cell that expressed only TRPC5. The currents were elicited by 100 μ M CCh. Compound **28** decreased the CCh-evoked currents. **C** & **D**, Current amplitudes immediately before (Control, Cntl) and at the end of the application of compound **28** (+**28**) for TRPC4 and TRPC5 at +100 mV (**C**) and -100 mV (**D**). Data are means \pm SEM for 5 TRPC4-expressing and 7 TRPC5-expressing cells. * $P < 0.05$, ** $P < 0.01$ vs Cntl by paired t test. **E** & **F**, % inhibition of agonist-evoked currents by compounds **9**, **13**, and **28** for TRPC4 and TRPC5 under the same protocol as shown in **A** & **B** at +100 mV (**E**) and -100 mV (**F**). Data (means \pm SEM) for compound **28** were derived from **C** & **D**. Data for compounds **9** and **13** were from separate experiments using cells that co-expressed μ OR with either TRPC4 β or TRPC5. Currents were elicited by costimulation with DAMGO (0.1 μ M) and CCh (10 μ M). Numbers of cells are indicated in parentheses. **

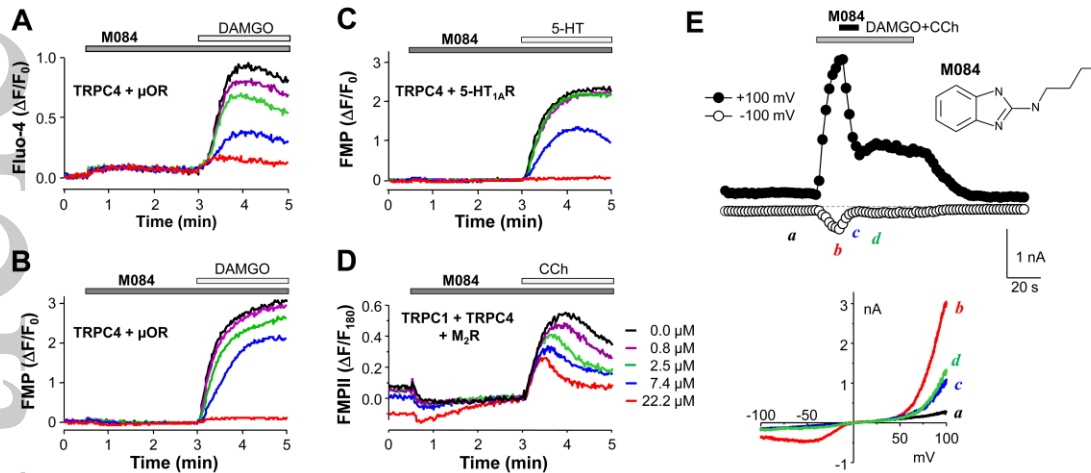
$P < 0.01$, *** $P < 0.001$ by one sample t tests comparing to 100% (no inhibition). **G**, Compound **28** inhibited riluzole-induced TRPC5 currents. Similar to **B**, but riluzole (50 μM) was applied to elicit TRPC5 currents. Summary data (means \pm SEM, $n = 6$) for current amplitudes immediately before (Cntl) and at the end of compound **28** (10 μM) application (+**28**) are shown at right. *** $P < 0.001$ vs Cntl by paired t test. **H**, Similar to **G**, but the cells expressed TRPC1, TRPC4 β and M₂R, and currents were evoked by CCh (10 μM). Summary data also represent $n = 6$ cells.

Figure 5 | Pretreatment with compound 28 suppressed activation of TRPC4 and TRPC5 but not TRPC6 by agonist stimulation. A-C, Currents evoked by DAMGO (0.1 μM) and CCh (30 μM) in cells that co-expressed TRPC4 β and μOR without (**A**) or with (**B**) a pretreatment by compound **28** (10 μM) for ~30 sec. Compound **28** was also present throughout the exposure to the agonists. Shown are time courses of currents at +100 and -100 mV (*left*) and I-V relationships obtained by the voltage ramp protocol (same as Fig. 4A) before (*black trace*) and during (*red trace*) agonist stimulation (*right*). Summary data (means \pm SEM) for agonist-induced peak current amplitudes (absolute values) at +100 and -100 mV are shown in **C**. $n = 7$ for control, $n = 5$ for +**28**. ** $P < 0.01$. *** $P < 0.001$ vs control by unpaired t test. **D-F**, Similar to **A-C**, but the cells expressed TRPC5 and the agonist was CCh (100 μM). Note the decrease of basal current at +100 mV upon application of compound **28** (**E**). The I-V curve for basal current before addition of compound **28** (*gray trace*) is indicated by the solid arrow, while that for current in the presence of compound **28** but before CCh (*black trace*) is indicated by the open arrowhead. For summary in **F**, $n = 7$ for control, $n = 6$ for +**28**. * $P < 0.05$. *** $P < 0.001$ vs control by unpaired t test. **G-I**, Similar to **A-C**, but the cells co-expressed TRPC6 and M₃R and the agonist was CCh (3 μM). For summary in **I**, $n = 6$ for control, $n = 6$ for +**28**.

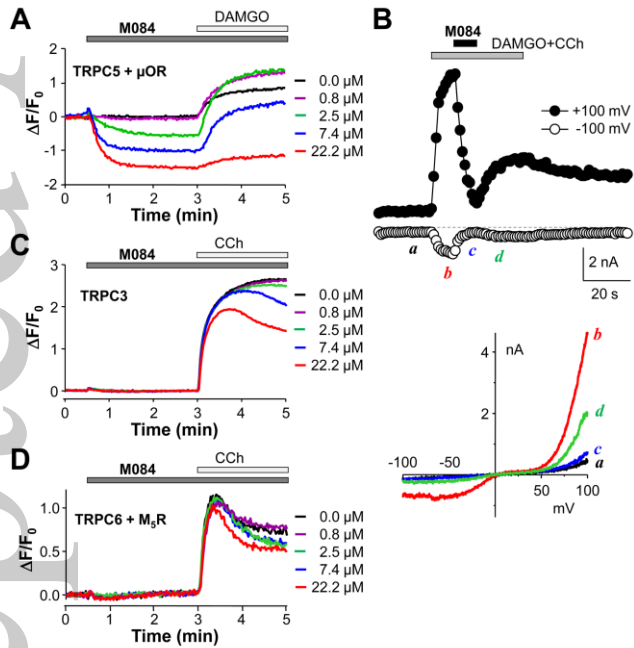
Figure 6 | M084 and analogs did not inhibit other channels. A-D, Compound **28** had no effect on TRPA1, TRPM8, TRPV1, and TRPV3. HEK293 cells stably expressing human TRPA1 (**A**), mouse TRPM8 (**B**), mouse TRPV3 (**D**) or transiently expressing rat TRPV1 (**C**) were seeded in wells of 96-well plates, loaded with Fluo-4, and read in a microplate reader for changes in $[\text{Ca}^{2+}]_i$. Compound **28** (7.4 and 22.2 μM) or buffer alone (0 μM) was added as indicated for 2.5 min before the application of the corresponding agonist: flufenamic acid (FFA, 100 μM , **A**), menthol (200 μM , **B**), capsaicin (1 μM , **C**), 2-aminoethoxydiphenyl borate (2APB, 200 μM , **D**). **E**, Summary (means \pm SEM) for agonist-induced Fluo-4 fluorescence changes in cells that expressed TRPA1, TRPM8, TRPV1, and TRPV3 in the presence of 22.2 μM **M084** and its analogs, compounds **9**, **13**, **27**, and **28**. Agonists and their concentrations are the same as shown in **A-D**. Integrated fluorescence changes (area under the curve) were normalized to that in the absence of the 2-aminobenzimidazole drug (control). $n = 6$ measurements for each. Only compound **27** showed moderate inhibition of TRPA1 and TRPM8. * $P < 0.05$ vs corresponding control. **F**, Representative current traces of voltage-gated Na⁺, K⁺, and Ca²⁺ channels (I_{Na} , I_{K} , I_{Ca}) before (*black traces*) and during (*red traces*) the application of **M084** (30 μM) and after

its washout (*blue traces*), recorded from dissociated mouse dorsal root ganglion neurons. Voltage protocols are shown above the traces. Current traces are overlaid for comparison, with the one during **M084** application placed in the front. Histogram shows means \pm SEM of current densities, at step voltages that yielded the maximal currents, in the presence of **M084** normalized to the average values before **M084** and after washout to correct for run-down in some cells. Numbers of cells tested are shown in parentheses.

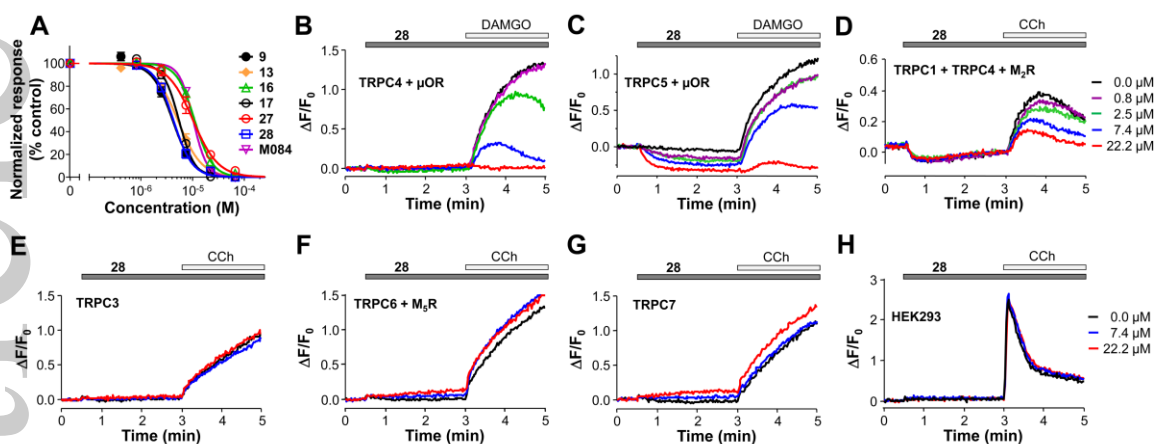
Figure 7 | M084 and analogs inhibited TRPC4-mediated plateau potentials in lateral septal neurons. **A**, Plateau potentials evoked by pressure ejection of DHPG (30 μ M) and concomitant current injection in lateral septal neurons. The lateral septal neuron in mouse brain slice was held at -80 mV under whole-cell current clamp mode. A series of 9 current injections (20 ms, 0.2-1 nA, with a 0.1-nA increment and 1.3 s intervals) were applied immediately before initiation of DHPG ejection (5-20 psi, 30 ms) (current protocol and time of DHPG application, indicated by the gray bar, shown in *upper panel*). Traces from all 9 sweeps are overlaid, with the one that yielded the maximal depolarization response shown in black (*lower panel*). **B-F**, Similar to **A**, but DHPG was co-ejected with **ML204** (**B**), **M084** (**C**), compound **9** (**D**), **13** (**E**), or **28** (**F**). **G**, Summary of maximal depolarization response, as determined by area under the trace from the sweep with the longest depolarization period. Data are means \pm SEM for the numbers of neurons indicated in parentheses. All drugs were used at 30 μ M except for **M084**, which was used at 100 μ M. * $P < 0.05$, ** $P < 0.01$, compared to DHPG alone.



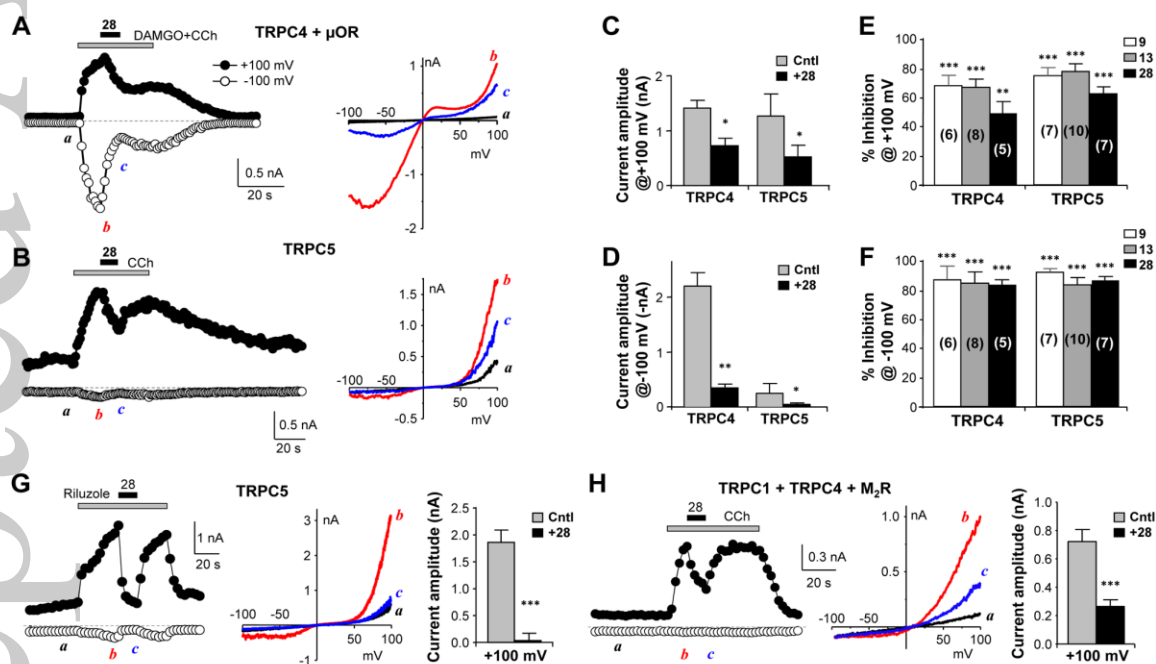
Zhu et al., Figure 1



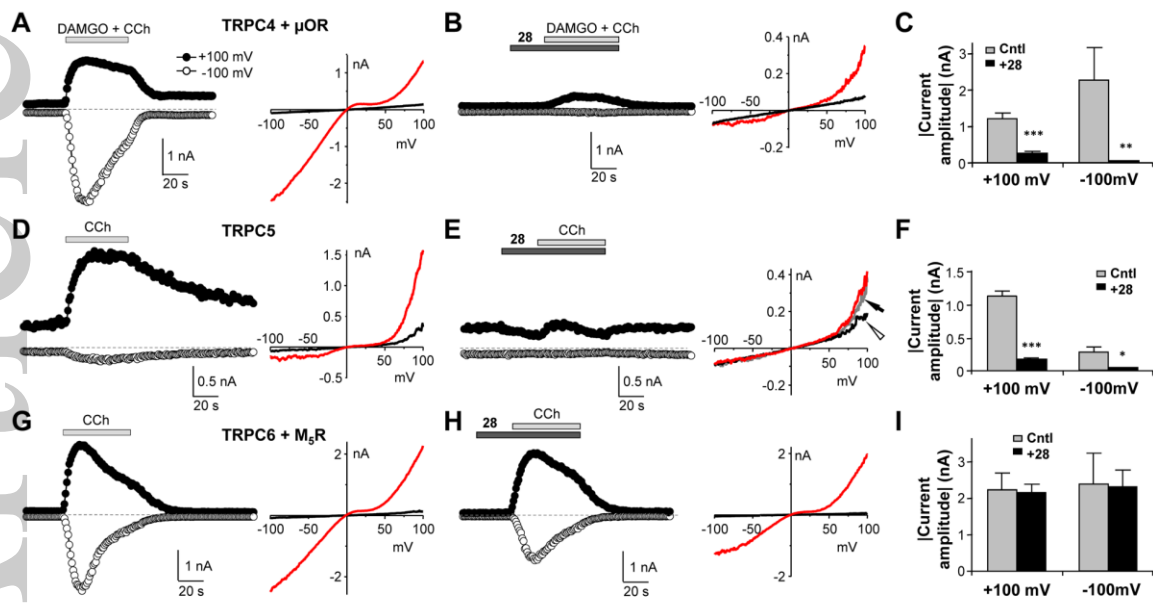
Zhu et al., Figure 2



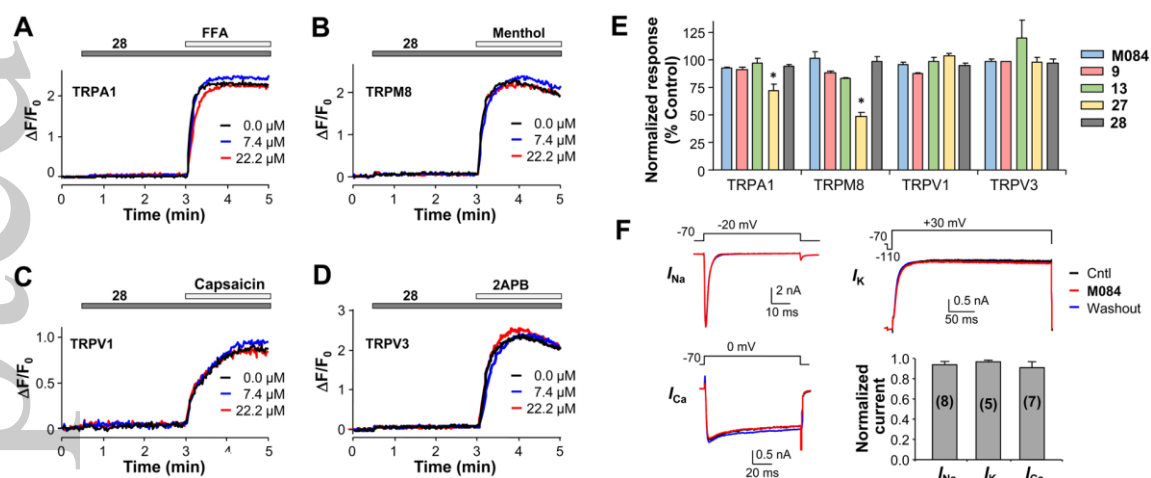
Zhu et al., Figure 3



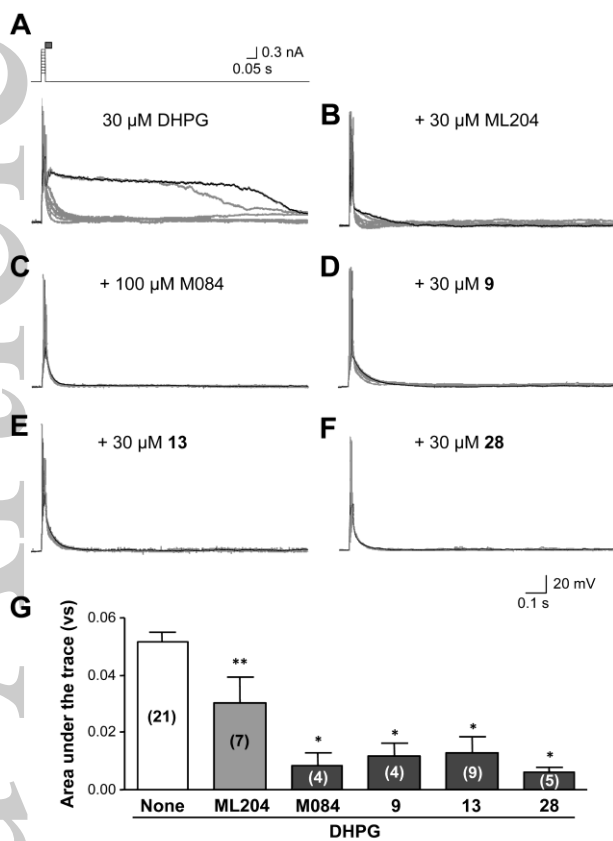
Zhu et al., Figure 4



Zhu et al., Figure 5

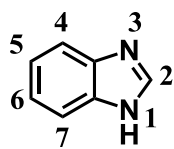


Zhu et al., Figure 6



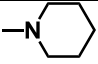
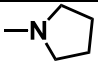
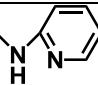



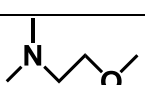

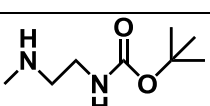
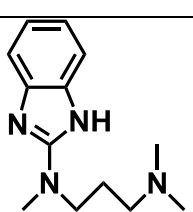

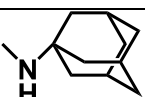
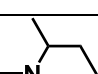
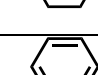
Zhu et al., Figure 7

Table 1. SAR evaluation of benzimidazole derivatives on TRPC4



Benzimidazole backbone

Compound	Position 2	Position 1	Position 5	Source	Inhibition @ 22 μ M
M084		-H	-H	Resynthesized	93%
2	-NH ₂	-H	-H	SA: 171778	No
3		-H	-H	SA: 572721	No
4		-H	-H	SA: L200263	13%
5	-NH ₂		-H	SA: L202517	24%
6		-H	-H	SA: S441503	No
7		-H	-H	SA: S62597	No
8			-H	SA: T320684	21%
9		-H	-Cl	SA: T320722	92%
10		-H	-Cl	SA: T135674	No
11		-H	-Cl	SA: T320625	No
12		-H	-Cl	SA: T320633	No
13		-H	-H	SA: T320676	94%
14		-H	-H	CB: 4003377	No
15		-H	-H	CB: 4033874	No

16		-H	-H	CB: 4034369	87%
17		-H	-H	CB: 4034623	95%
18		-H	-H	New Synthesis	No
19		-CH ₃	-H	New Synthesis	No
20		-CH ₃	-H	New Synthesis	No
21		-H	-H	New Synthesis	No
22		-H	-H	New Synthesis	No
23		-H	-H	New Synthesis	No
24		-H	-H	New Synthesis	No
25		-H	-H	New Synthesis	No
26		-H	-H	New Synthesis	31%
27		-H	-H	New Synthesis	80%
28		-H	-H	New Synthesis	97%
29		-H	-H	New Synthesis	No

SA: Sigma Aldrich, CB: ChemBridge

Functional assay performed by fluorescence membrane potential measurements of DMAGO-evoked response in cells co-expressing TRPC4 β and μ OR.

Table 2. IC₅₀ values (μM) of 2-aminobenzimidazole compounds on TRPC3/C4/C5/C6

	TRPC4β+μOR (vs DAMGO)	TRPC5+μOR (vs DAMGO)	TRPC6+M ₅ R (vs CCh)	TRPC3 (vs CCh)
M084	10.3 ± 0.5 (n = 12)	8.2 ± 0.7 (n = 12)	59.6 ± 16.3 (n = 6)	48.6 ± 9.5 (n = 6)
9	4.1 ± 0.6 (n = 12)	3.1 ± 0.5 (n = 12)	57.1 ± 9.5 (n = 6)	30.4 ± 5.3 (n = 6)
13	5.2 ± 0.7 (n = 12)	6.6 ± 0.9 (n = 12)	63.8 ± 17.1 (n = 6)	19.3 ± 0.6 (n = 6)
16	11.0 ± 1.0 (n = 12)	11.1 ± 1.1 (n = 6)	>100 (n = 6)	>100 (n = 6)
17	5.5 ± 0.5 (n = 12)	8.0 ± 1.0 (n = 6)	>100 (n = 6)	>100 (n = 6)
27	10.2 ± 1.4 (n = 12)	12.4 ± 1.3 (n = 6)	>100 (n = 6)	>100 (n = 6)
28	4.3 ± 0.4 (n = 12)	3.5 ± 0.3 (n = 6)	>100 (n = 6)	>100 (n = 6)

Fluorescence membrane potential measurements on stable TRPC cell lines were performed as in Fig. 3 using either FMP or FMP II. Agonist evoked fluorescence increases (area under the curve) were normalized to that from the control pretreated with the buffer alone. For TRPC5, the remaining fluorescence intensity in the highest concentration of the antagonist for each set of the experiments was assumed to represent no activity and used for baseline subtraction for calculating the area under the curve. Data points were fitted with the Hill equation to determine IC₅₀ values, expressed as means ± SEM for the numbers of measurements indicated in parentheses.